Journal of Ambient Intelligence and Humanized Computing
https://doi.org/10.1007/s12652-020-01722-8

ORIGINAL RESEARCH

Classification of epileptic electroencephalogram signals using tunable-Q wavelet transform based filter-bank

Anurag Nishad[1] · Ram Bilas Pachori[1]

Received: 30 March 2018 / Accepted: 17 January 2020
© Springer-Verlag GmbH Germany, part of Springer Nature 2020

Abstract

The epilepsy is a neurological disorder and the seizure events frequently appear in epileptic patients. This disorder can be analysed through electroencephalogram (EEG) signals. In this paper, we propose a novel approach for automated identification of seizure EEG signals. The proposed method in this paper decomposes EEG signal into set of sub-band signals by applying tunable-*Q* wavelet transform (TQWT) based filter-bank. The sub-bands in TQWT based filter-bank have different value of quality (*Q*)-factor and have nearly constant bandwidth (*BW*). The features are computed by applying cross-information potential (CIP) on N_s number of sub-band signals, for N_s values varying from two to maximum number of sub-band signals obtained from TQWT based filter-bank. The features are computed for various values of N_s and fed as input to random forest (RF) classifier. We have observed that, with the increase in the N_s, the number of computed features increases and hence the classification accuracy (ACC) depends on N_s. In this work, we have obtained ACC of 99% in the classification of normal, seizure-free, and seizure EEG signals using our proposed method. The developed algorithm is ready to be tested using huge database and can be employed to aid the epileptologists to screen the seizure-free and seizure patients accurately.

Keywords Epilepsy · Electroencephalogram signal · Tunable-Q wavelet transform · Cross-information potential · Random forest classifier · Epileptic seizure classification

1 Introduction

Almost sixty million people throughout the world are affected with epilepsy disorder and most of them belong to the developing countries (Witte et al. 2003). Inside human brain of epileptic patient, the epilepsy occurs which is the neurological disorder. During epilepsy, seizure events occur frequently. To analyse the neurological activity of brain, the electroencephalogram (EEG) signals are commonly used. The EEG signals are the electrical activity of brain and it was first observed by Caton in 1875 (Caton 1875). Later, in 1929, Hans Berger experimentally showed the presence of EEG signals by placing galvanometer connected electrodes on the head (Berger 1929). Since then, EEG signals are used in many research areas including the diagnosis of epilepsy (Peker et al. 2016). However, it is difficult and time-consuming for the neurologists to detect the epileptic seizure visually. Therefore, many automated techniques using advanced signal processing algorithms have been proposed to detect epileptic seizures (Bhattacharyya et al. 2017b; Sharma and Pachori 2015; Bajaj and Pachori 2012). These techniques classify and detect epileptic seizure based on the extracted features from the EEG signals.

In this paper, we address the classification of seizure, seizure-free, and normal EEG signals. The EEG signals are non-stationary in nature and hence it would be better if they are decomposed into less complex signals. The seizure, seizure-free, and normal EEG signals have different characteristics (Andrzejak et al. 2001). Therefore, it gives us motivation to classify EEG signals by decomposing them into set of sub-band signals. Then by selecting optimum number of sub-band signals and capturing similarity among these sub-bands would result in good classification accuracy (ACC). Therefore, we employed a tunable-*Q* wavelet transform (TQWT) based filter-bank (Pachori and Nishad 2016; Nishad et al. 2018) to decompose EEG signals. The TQWT based filter-bank contains nearly constant bandwidth (*BW*) sub-bands which are obtained from different quality (*Q*)-factor values. These different *Q*-factor values generate various

✉ Anurag Nishad
phd1401202003@iiti.ac.in

[1] Discipline of Electrical Engineering, Indian Institute of Technology Indore, Indore 453552, India

mother wavelets, which are suitable to analyse different EEG signals which vary in oscillatory nature since they are non-stationary (Boashash et al. 2003). If different EEG signals of different oscillatory nature are decomposed by TQWT, then this implies that only single value of Q-factor is used. Then, there is need to determine optimum value of Q-factor for decomposing different EEG signals. This is because only one value of Q-factor is not suitable to analyse both low and high oscillatory signals (Selesnick 2011b).

After decomposition of EEG signals by TQWT based filter-bank, the cross information potential (CIP) is applied on sub-band signals to compute features. The CIP captures the similarity between two random variables (Xu et al. 2008). The motivation, novelty, and contribution of this work are as follows:

1. Motivation: Different class of EEG signals has different characteristics (Andrzejak et al. 2001). Hence, there is a motivation to develop an automated system to classify different EEG signals based on these characteristics.
2. Novelty: The application of TQWT based filter-bank for signal decomposition and CIP for features computation are the novelties of this work.
3. Contribution: The TQWT based filter-bank decomposes EEG signal into narrow BW sub-band signals. Hence the CIP feature computation from narrow BW sub-band signals is the contribution of this work.

The rest of paper is organized as follows: the literature review is presented in Sect. 2 and the overview of TQWT is presented in Sect. 3. Section 4 describes the proposed methodology which includes description of design of TQWT based filter-bank, method to compute features, and classifier used in this work. Then the Sect. 5 is the experimentation which describes the dataset used. The simulation results are presented in Sect. 6. The Sect. 7 presents the discussion and finally Sect. 8 concludes the paper.

2 Literature review

In literature, there are many studies presented for the diagnosis of epilepsy through EEG signals. These studies perform detection and classification of EEG signals. Generally, the classification problems which are dealt in literature are classification of seizure and seizure-free EEG signals, classification of seizure and non-seizure EEG signals, classification of seizure and normal EEG signals, and classification of seizure, seizure-free, and normal EEG signals. The seizure EEG signals are recorded during seizure activities and seizure-free EEG signals are recorded when seizure activities are absent from the patient suffering from epilepsy (Andrzejak et al. 2001). The normal EEG signals are recorded from healthy subjects and non-seizure EEG signals include both normal and seizure-free EEG signals (Andrzejak et al. 2001). These classifications can be performed by extracting features from EEG signals. The features can be extracted in frequency-domain, time-domain, time–frequency (T–F) domain, or by non-linear signal analysis methods.

Due to non-stationary nature of EEG signals Boashash et al. (2003), the features in T–F domain can be extracted. In Sharma and Pachori (2018), the authors proposed improved eigenvalue decomposition of Hankel matrix and Hilbert transform (IEVDHM-HT) based T–F representation to analyse the non-stationary signals. The proposed T–F representation in Sharma and Pachori (2018), has been used to classify seizure-free and seizure EEG signals. The size of Hankel matrix used in T–F representation would be more if the signals length is large. The complexity of the system increases due to this factor. In Samiee et al. (2015), the features used to classify seizure and non-seizure EEG signals are extracted from rational discrete short time Fourier transform (STFT) and then multilayer perceptron (MLP) classifier is used as classifier. The T–F based methods along with artificial neural network (ANN) were used to classify epileptic seizure from EEG signals (Tzallas et al. 2007, 2009). Different T–F distributions are considered in (Samiee et al. 2015; Tzallas et al. 2007, 2009). The performance analysis of non-stationary signal like EEG may be affected by the choice of T–F distribution. Since, these distributions differ in terms of their T–F localization and complexity. Therefore T–F distribution with good localization and less complexity should be chosen to analyze the EEG signals in T–F domain. There are different kinds of T–F distributions are considered in Samiee et al. (2015); Tzallas et al. (2007, 2009). Different T–F distributions differ in terms of localization and complexity. The features based on time and frequency domain are used to detect epileptic seizure EEG signals as shown in Srinivasan et al. (2005); Polat and Gunes (2007). However, in these methods, the non-stationary nature of EEG signals is not considered.

In non-linear signal analysis methods, classification of seizure EEG signals have been performed using nonlinear parameters as features. The correlation dimension (Lehnertz and Elger 1995), fractal dimension (Accardo et al. 1997; Patidar et al. 2015a), Lyapunov exponent (Guler et al. 2005; Ubeyli 2010), Higher order spectra (HOS) (Acharya et al. 2011b), continuous wavelet transform (CWT) (Acharya et al. 2013), recurrence quantification analysis (RQA) (Acharya et al. 2011a), Hurst exponent (Acharya et al. 2009), approximate entropy (ApE) (Liang et al. 2010), sample entropy (SaE) and phase entropy (Acharya et al. 2012) are the various nonlinear features used for the seizure detection with EEG signals. However, there is need to find the suitable nonlinear parameter which can provide significant information for accurate classification, since they are applied directly on the EEG signals.

Since the nature of EEG signal is non-stationary (Boashash et al. 2003), there are many studies presented in which features are extracted after the decomposed EEG signals. The empirical mode decomposition (EMD) has been used to decompose EEG signals (Sharma and Pachori 2015) into set of intrinsic mode functions (IMFs). Then features based on phase space representation (PSR) of IMFs are obtained for classification of seizure-free and seizure EEG signals. Similarly in Pachori and Patidar (2014), 95% confidence area of ellipse has been computed from second order difference plot (SODP) of IMFs and used as feature to classify seizure and seizure-free EEG signals. Similarly in Pachori et al. (2015), classification of normal and seizure EEG signals is shown. The Fourier-Bessel series expansion has been used to compute the mean frequency of IMFs (Pachori 2008). The mean frequency is used as feature to classify seizure-free and seizure EEG signals. Also in Oweis and Abdulhay (2011), the weighted mean frequency of IMFs are introduced to find epileptic seizure EEG signals. From the plots of analytic IMFs, area used to classify seizure and normal EEG signals (Pachori and Bajaj 2011). In Bajaj and Pachori (2012), the non-seizure and seizure EEG signals are classified by feature set obtained by frequency modulation (FM) and amplitude modulation (AM) *BWs* of IMFs. These methods make use of EMD for signal decomposition. However, the EMD suffers from mode-mixing problem which is the presence of intermittency at some part of the signal (Oweis and Abdulhay 2011; Huang et al. 1999). Due to this mode-mixing, it is hard to predict whether different time-scale oscillations occur in a single mode or oscillation of constant time scale given to different modes (Oweis and Abdulhay 2011).

Apart from EMD, the wavelet transform has been used for signal decomposition in various methods. In Subasi and Gursoy (2010), the EEG signal is decomposed into number of sub-bands by applying discrete wavelet transform (DWT) and then statistical features are computed from sub-bands. Then, support vector machine (SVM) after data dimension reduction, has been applied for classification of normal and seizure EEG signals. Similar classification problem is addressed in Lee et al. (2014), where features have been computed from Euclidean distance, which are computed from wavelet coefficients. In Orhan et al. (2011), the DWT is used to decompose EEG signal into sub-bands. Then clustering of wavelet coefficients using *k*-means algorithm is accomplished for each sub-bands. Using distribution of wavelet coefficients, the probability distributions were computed and fed as input to MLP neural network (MLPNN). The DWT is unable to differentiate input signal changes and the phase information of signal is absent (Peker et al. 2016). To overcome these limitations, the authors in Peker et al. (2016), extracted features from EEG signals using dual tree complex wavelet transform (DTCWT). Then, complex valued neural networks is used for diagnosis of epilepsy. Also in Chen (2014), DTCWT and Fourier features have been used to detect seizure by using nearest neighbor classifier. Other wavelet transform and multi-wavelet transform based techniques for classification and detection of epileptic seizure can be found in Adeli et al. (2003, 2007); Ghosh-Dastidar et al. (2007); Khan and Gotman (2003); Ocak (2009); Subasi (2007); Guo et al. (2010). In Patidar and Panigrahi (2017), the EEG signals are decomposed into sub-bands by applying TQWT and features were obtained by applying Kraskov entropy. The least squares SVM (LS-SVM) classifier to classify seizure and seizure-free EEG signals is used by author. The application of TQWT to decompose EEG signals can also be found in Hassan et al. (2016), where authors classify normal, seizure-free, and seizure EEG signals by using bagging classifier. Similarly in Sharma and Pachori (2017), authors applied TQWT to decompose EEG signals and computed fractal dimension as feature to address various kinds of classification problems. In Bhattacharyya et al. (2017b), EEG signals are decomposed by TQWT and then K-nearest neighbor (K-NN) based entropies were estimated in order to classify epileptic EEG signals. These methods which used TQWT to decompose the EEG signals need to find optimum value of *Q*-factor before decomposition. This is because a *Q*-factor defines a mother wavelet which is not suitable to analyse signals of different oscillatory nature (Selesnick 2011b). In Bhati et al. (2017b) and Bhati et al. (2017a), optimal wavelet filter-banks are designed to classify seizure-free and seizure EEG signals.

3 Tunable-*Q* wavelet transform

The TQWT is a kind of wavelet transform which provides the option to vary the *Q*-factor of wavelet. For different *Q*-factor, different mother wavelets can be obtained. For high oscillatory signal, the *Q*-factor of TQWT can be set to high value and for low oscillatory signal, the *Q*-factor can be set to low value (Selesnick 2011b). Such option is not present in the conventional wavelet transform. The TQWT decomposes the EEG signal for a particular value of *Q*-factor. A single value of *Q*-factor, may not be suitable for the classification of different EEG signals which differ in oscillatory behaviour. Therefore, TQWT based filter-bank can be used in place of TQWT, in which EEG signals would be decomposed by many *Q*-factors simultaneously. The sub-bands in TQWT based filter-bank has nearly same and narrow *BW*. Therefore, the entire frequency range of EEG signal is distributed among these narrow *BW* sub-bands. Hence, the energy of EEG signal is disperse among these narrow and constant *BW* sub-band signals. Then, optimum number of narrow *BW* sub-band signals can be selected for classification.

Other than Q-factor, there are two more parameters available in TQWT, namely level of decomposition (L) and redundancy factor (r). The parameter L determines the number of sub-bands into which input signal will be decomposed (Selesnick 2011b). It's value can be increased to decompose the input signal into more number of sub-bands in low frequency range (Patidar et al. 2015b). The value of r controls the overlapping among adjacent sub-bands in frequency-domain (Patidar et al. 2015b). High value of r increases the overlapping among sub-bands and increases the time-domain localization of wavelet (Patidar et al. 2015b).

The building block to implement TQWT is a two channel filter bank (TCFB). The TCFB has one input and two outputs corresponding to two channels. The first channel is low pass channel (LPC) which consists of a low pass filter (LPF), followed by a scaling factor, SL. Similarly second channel is high pass channel (HPC) which includes a high pass filter (HPF), followed by a scaling factor, SH (Selesnick 2011b). To implement TQWT, the output of LPC is given as input to another TCFB. In this way, many TCFBs can be connected in iterative way (Selesnick 2011b). As shown in Fig. 1, a signal is given as input to first TCFB. Apart from input signal, TQWT parameters are also given as input to the TQWT. The value of SL and SH is computed from the value of TQWT parameters Q-factor, r, and L and their relation is given as follows (Selesnick 2011b):

$$\mathrm{SL} = 1 - \frac{\mathrm{SH}}{r} \tag{1}$$

$$\mathrm{SH} = \frac{2}{Q+1} \tag{2}$$

However, there are conditions on the values of SL and SH (Selesnick 2011b) and TQWT can be applied only when these conditions are not violated. The values of scale factors should be between zero and one, so that wavelet transform do not become redundant (Selesnick 2011b). Also the sum of their values should be greater than one in order to achieve localization of time-domain response of LPF and HPF (Selesnick 2011b). The Fig. 1 is valid only when these conditions on scale factors are satisfied.

The output from HPC of each TCFB is a sub-band (Selesnick 2011b). If L number of TCFBs are connected in iterative way, then there will be $L+1$ sub-bands as shown in Fig. 1. This is because output from LPC and HPC of last TCFB are considered as sub-band.

Fig. 1 Illustration of sub-band decomposition based on TQWT method

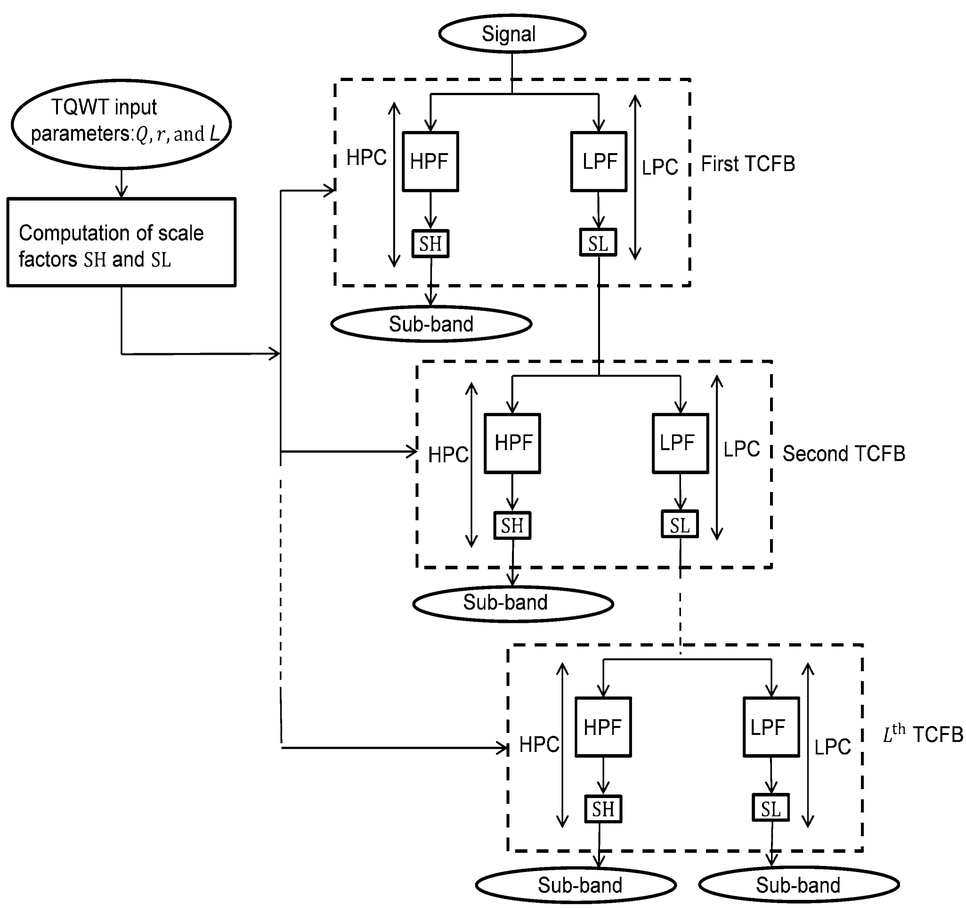

The TQWT has been applied in the classification and analysis of various biomedical signals. Its application can be found in detection of focal (Sharma et al. 2017; Bhattacharyya et al. 2017a) and alcoholic (Patidar et al. 2017) EEG signals, etc.

4 Proposed Method

The proposed method for classification of normal, seizure-free, and seizure EEG signals consists of three stages. The Fig. 2 shows the block diagram of proposed method. First stage in block diagram is decomposition of EEG signals by TQWT based filter-bank. The second stage is feature computation from decomposed signals and final stage is classification of EEG signals using a classifier. These stages are described below.

4.1 TQWT based filter-bank

The frequency response of TQWT can be obtained by specifying the values of Q-factor, r, and L. In frequency response, there will be L sub-bands obtained from each HPC of TCFB and one sub-band from LPC of Lth TCFB (Selesnick 2011b). The BW and center frequency (F_c) of each sub-band will be different but the ratio F_c to BW of each sub-band is constant. This ratio is equal to the Q-factor (Selesnick 2011b). The F_c and BW of each sub-band depends on scale factors SL and SH and their relations for l^{th} sub-band is given as follows (Selesnick 2011b):

$$F_c = (\mathrm{SL})^l \left(\frac{2 - (\mathrm{SH})}{4(\mathrm{SL})} \right) F_s \tag{3}$$

$$BW = \frac{(\mathrm{SH})(\mathrm{SL})^{l-1}\pi}{2} \tag{4}$$

The sampling frequency of signal is F_s and $1 \le l \le L + 1$. Our aim is to design a filter-bank whose frequency response consists of narrow and nearly constant BW sub-bands. The TQWT based filter-bank in proposed method is designed manually. To construct TQWT based filter-bank, the following steps can be followed:

1. Choose a constant BW for all sub-bands in TQWT based filter-bank.
2. Select F_c of first sub-band of TQWT based filter-bank which is the lowest F_c sub-band in TQWT based filter. Therefore it's F_c should be minimum.
3. Set $l = L$ in (3) and (4). In this way, we will only examine the F_c and BW of sub-band generated from HPC of L^{th} TCFB as shown in Fig. 1.
4. At this step, we have five variables and four equations. The variables are Q-factor, r, L, SL, and SH and equations are (1), (2), (3), and (4). Set r equals to a constant. In this way, we reduce our problem to four variables and four equations. In these equations, we set the desired value of F_c and BW. It should be noted that $r \ge 3$ (Selesnick 2011b). In the proposed method, $r = 9$ is chosen.
5. Replace variables SL and SH in (3) and (4) in terms of Q-factor and r from (1) and (2). Then value of Q-factor and L are set manually such that the obtained F_c and BW are as close to desired values of F_c and BW, respectively. It should be noted that the value of L should be positive integer only.
6. Repeat above mentioned steps for other subsequent sub-bands in TQWT based filter-bank. Note that the F_c of sub-band must not exceed 0.5 (normalized frequency).

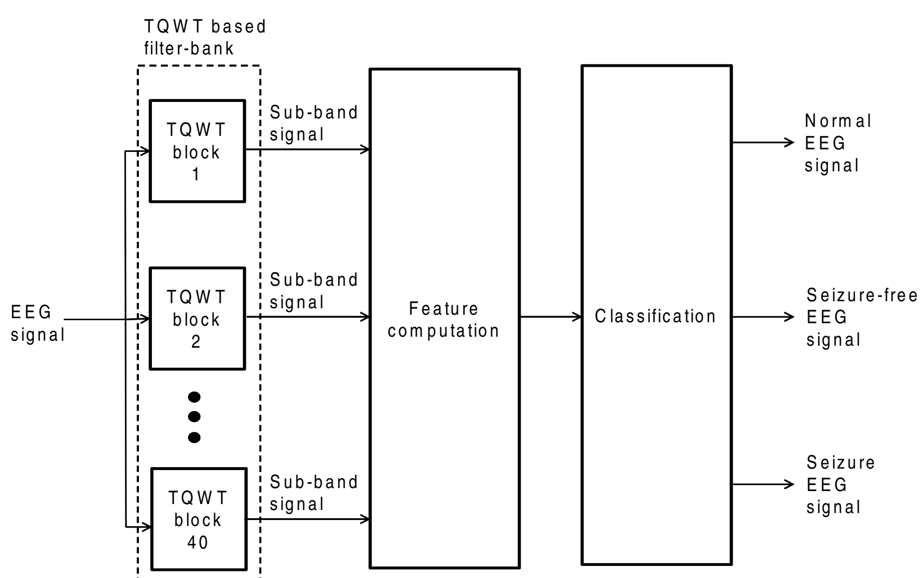

Fig. 2 Block diagram for the detection of epileptic EEG signals

The F_c of first sub-band is set to 0.03 (normalized frequency) and F_c of adjacent sub-bands differ by approximately 0.01 (normalized frequency). The designed TQWT based filter-bank which is used in this work is shown in Fig. 3.

In Fig. 3, the normalized gain is the frequency response of sub-band divided by it's maximum value. In this way, the maximum value of normalized gain is one. The normalized frequency is the frequency of the signal divided by F_s. According to Nyquist sampling theorem, the F_s must be atleast two times of the maximum frequency present in the signal. Therefore maximum value of normalized frequency cannot exceed 0.5.

In Fig. 2, the TQWT based filter-bank is shown using many TQWT blocks. The number of TQWT blocks is equal to the number of sub-bands in TQWT based filter-bank. The obtained value of Q-factor, r, and L for particular sub-band is assigned to its corresponding TQWT block. Each TQWT block applies wavelet transform on input signal. Then the wavelet coefficients of each sub-band except wavelet coefficients of sub-band generated from HPC of L^{th} TCFB are set to zero. In the next step, inverse TQWT is applied in order to obtain a sub-band signal (Selesnick 2011a). In this way, each TQWT block produces a sub-band signal and input signal is decomposed into these sub-band signals.

The sub-band 1 as shown in Fig. 3 is the lowest F_c sub-band among the sub-bands present in TQWT based filters. Then F_c of subsequent sub-bands increases gradually. There are total 40 sub-bands and the BW of each sub-band in frequency response of TQWT based filter bank is nearly 0.025 (normalized frequency). The chosen values of Q-factor, r, and L in each TQWT block are mentioned in the results section. During simulation, sub-band signals from sub-band 1 to sub-band N_s are chosen for classification by varying the value of N_s from $N_s = 2$ to 40.

4.2 Feature computation

After decomposition of EEG signal by TQWT based filter-bank, the CIP (Xu et al. 2008) is used to obtain features. The information potential (IP) estimates the Renyi's quadratic entropy. If it is applied on a sub-band signal then it can be expressed as (Xu and Erdogmuns 2010):

$$\text{IP}(SB_i) = \frac{1}{T^2} \sum_{ia=1}^{T} \sum_{ib=1}^{T} R(SB_{ia} - SB_{ib}) \tag{5}$$

where, T is the total number of samples in sub-band signal SB_i and $R(SB_{ia} - SB_{ib})$ is the kernel function. The a^{th} and b^{th} sample of sub-band signal SB_i is represented by SB_{ia} and SB_{ib}, respectively. The CIP measures the similarity between two probability density functions (PDFs) (Xu et al. 2008) and can be expressed as follows:

$$\text{CIP}(SB_i, SB_j) = \frac{1}{T^2} \sum_{ia=1}^{T} \sum_{jb=1}^{T} R(SB_{ia} - SB_{jb}) \tag{6}$$

where SB_{ia} is the a^{th} sample of sub-band signal SB_i and SB_{jb} is the b^{th} sample of sub-band signal SB_j. In the proposed method, the CIP is computed between i^{th} sub-band signal SB_i and j^{th} sub-band signal SB_j, where $1 \leq i \leq N_s, 1 \leq j \leq N_s$, and $i \neq j$. Also, there will be $\frac{N_s(N_s-1)}{2}$ number of CIPs computed if N_s number of sub-bands are considered in the simulation. In this work, the CIP is computed using ITL toolbox which can be downloaded from http://www.sohanseth.com/Home/codes. The incomplete Cholesky decomposition is used by ITL toolbox to compute CIP. The kernel size is set equal to two in classification problem. The analysis of physiological signal using CIP can be found in (Kumar et al. 2017) in which diagnosis of CAD using electrocardiogram (ECG) signals is shown.

It is not necessary that all extracted features would be significant in classification. Therefore, after having $\frac{N_s(N_s-1)}{2}$ number of features from N_s sub-band signals, it is required

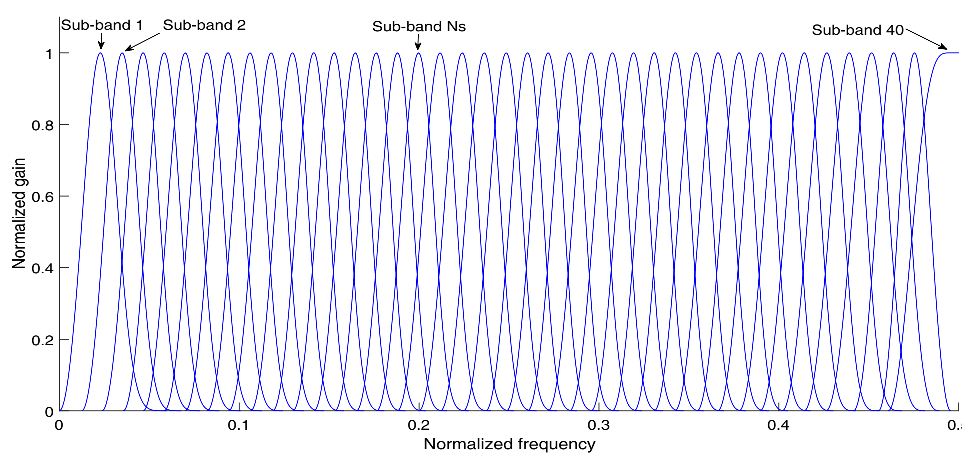

Fig. 3 TQWT based filter-bank used in our proposed method

to rank these features. The ranking of features is performed using RELIEFF algorithm (Kononenko et al. 1997; Robnik-Sikonja and Kononenko 2003). The RELIEFF algorithm estimates quality features according to their ability to discriminate instances which are close to each other (Kononenko et al. 1997; Robnik-Sikonja and Kononenko 2003). The algorithm randomly selects an instance. Then, it searches K-NNs which belongs to same class and K-NNs which belongs to other class (Kononenko et al. 1997; Robnik-Sikonja and Kononenko 2003). The significance of feature is determined by its quality estimation variable W which depends on the value of the instance and searched K-NNs belonging to same class and different class (Kononenko et al. 1997; Robnik-Sikonja and Kononenko 2003). In the proposed method, number of neighbour K in K-NN is set to one in RELIEFF algorithm.

After ranking the features, the highest ranked feature is used for classification. Then, next best two features are considered during classification and so on. In this way, the number of ranked features (NORF) given as input to the classifier is different in each step. Accordingly, the obtained ACC varies with the change in NORF.

4.3 Classification

The classifier used for classification is random forest (RF). The RF classifier (Breiman 2001) is based on several classification trees. The trees are generated according to random tree method as mentioned in (Fraiwan et al. 2012). To conduct classification, a weight is allotted to each tree and each tree individually performs classification of classes. The classification decision made by each tree is considered while performing the overall classification. In RF classifier, each tree has an assigned random vector. Let us say, the assigned vector to i^{th} tree is v_i. The assigned vectors are independent of each other, however their distribution is same. During classification, the class is determined by a margin function denoted by MF. The MF can be defined for a training set, which is picked randomly from random vector distribution G, H (Breiman 2001) as:

$$MF(H,G) = A(I[B(h,v_i) = G]) - \max_{j \neq G}(A(I[B(h,v_i) = j])) \tag{7}$$

where $B(h, v_i)$ is a tree classifier which depends on input training data h and assigned random vector v_i (Breiman 2001). $I[.]$ is a indicator function and A is the average value (Breiman 2001). The higher value of MF indicates more accurate classification (Breiman 2001). In this paper, the classification has been performed using Waikato environment for knowledge analysis (WEKA) software (Hall et al. 2009) and using ten-fold cross validation strategy.

5 Experimentation

The dataset used in this study is obtained from University of Bonn, Germany (Andrzejak et al. 2001). It is publicly available online database which contains EEG signals recorded from healthy and epileptic subjects. The duration and sampling frequency of each signal is 23.6 seconds and 173.67 Hz, respectively. The signals are categorized into five classes, namely Z, O, N, F, and S. Each class contains 100 EEG signals. The EEG signals of classes Z and O are the recorded from five healthy subjects using surface recording and standard 10-20 electrode placement system. The EEG signals from classes Z and O belong to normal EEG signals with eye open and closed respectively.

The class N and class F EEG signals are seizure-free signals since these signals are recorded in seizure-free interval. Class F EEG signals are recorded from epileptogenic zone and class N EEG signals are recorded from hippocampal portion of brain which is opposite to the hemisphere. Signals in class S carry seizure activities. In the study, class N and class F EEG signals are termed as seizure-free class and class S EEG signals are termed as seizure class.

6 Simulation results

The TQWT based filter-bank as shown in Fig. 3, is used to decompose EEG signals. The EEG signals are given as input to TQWT based filter-bank. The value of Q-factor in different TQWT block are as follows: $Q_1 = 1$, $Q_2 = 1.45$, $Q_3 = 1.87$, $Q_4 = 2.33$, $Q_5 = 2.72$, $Q_6 = 3.14$, $Q_7 = 3.58$, $Q_8 = 4.06$, $Q_9 = 4.56$, $Q_{10} = 5.1$, $Q_{11} = 5.68$, $Q_{12} = 6.1$, $Q_{13} = 6.56$, $Q_{14} = 7.04$, $Q_{15} = 7.56$, $Q_{16} = 7.87$, $Q_{17} = 8.2$, $Q_{18} = 8.56$, $Q_{19} = 8.93$, $Q_{20} = 9.63$, $Q_{21} = 10.37$, $Q_{22} = 10.8$, $Q_{23} = 11.28$, $Q_{24} = 11.4$, $Q_{25} = 11.93$, $Q_{26} = 12.5$, $Q_{27} = 13.1$, $Q_{28} = 13.8$, $Q_{29} = 13.94$, $Q_{30} = 14.1$, $Q_{31} = 14.98$, $Q_{32} = 15.17$, $Q_{33} = 15.4$, $Q_{34} = 15.6$, $Q_{35} = 15.9$, $Q_{36} = 16.2$, $Q_{37} = 16.5$, $Q_{38} = 19.5$, $Q_{39} = 23.7$, and $Q_{40} = 24.5$. Similarly, the value of L factor used in different TQWT blocks are $L_1 = 19$, $L_2 = 22$, $L_3 = 24$, $L_4 = 26$, $L_5 = 27$, $L_6 = 28$, $L_7 = 29$, $L_8 = 30$, $L_9 = 31$, $L_{10} = 32$, $L_{11} = 33$, $L_{12} = 33$, $L_{13} = 33$, $L_{14} = 33$, $L_{15} = 33$, $L_{16} = 32$, $L_{17} = 31$, $L_{18} = 30$, $L_{19} = 29$, $L_{20} = 29$, $L_{21} = 29$, $L_{22} = 28$, $L_{23} = 27$, $L_{24} = 25$, $L_{25} = 24$, $L_{26} = 23$, $L_{27} = 22$, $L_{28} = 21$, $L_{29} = 19$, $L_{30} = 17$, $L_{31} = 16$, $L_{32} = 14$, $L_{33} = 12$, $L_{34} = 10$, $L_{35} = 8$, $L_{36} = 6$, $L_{37} = 4$, $L_{38} = 3$, $L_{39} = 2$, and $L_{40} = 1$. The Q_i and L_i represent the value of Q-factor and L of i^{th} TQWT block. The value $r = 9$ is assigned to each TQWT block.

The value of N_s is varied from $N_s = 2$ to $N_s = 40$ and performance parameters namely, ACC, sensitivity (SEN), and specificity (SPE) (Azar and El-Said 2014) are observed corresponding to each value of N_s.

As shown in Fig. 3, there are 40 sub-bands in TQWT based filter-bank. If sub-band signals generated from all 40 sub-bands are considered in feature computation, then the complexity of the system would be very high. Therefore, we run the series of simulation in which features are computed from sub-band signals originated from sub-band 1 to sub-band N_s and in each simulation, the value of N_s is different. In first simulation run, the $N_s = 2$ is chosen since sub-band signals from at least two sub-bands are required to compute CIP. Then in subsequent simulations, the value of N_s is incremented by one. The maximum value of N_s is the number of sub-bands in TQWT based filter-bank. Then the features are ranked after feature computation and fed to the classifier. The best value of N_s or best set of N_s sub-band is one for which the classifier achieves maximum ACC. When N_s sub-bands are selected for classification, then there will be $\frac{N_s(N_s-1)}{2}$ number of features available because CIP is computed from every possible pair of sub-band signals obtained from N_s selected sub-bands. When the value of N_s is varied, then number of sub-band signals used in feature computation also changes. During the simulation, the proposed method is tested for different length of EEG segments. The segment length, which is considered during simulation are 500 samples, 1000 samples, 2000 samples, and entire length (4097 samples) of EEG signal. The obtained ACC for different segment length of EEG signal is shown in Table 1. The Table 1 shows the maximum obtained ACC when sub-band signals from minimum N_s sub-bands are used in feature computation and minimum NORF are used.

From Table 1, it can be noted that maximum obtained ACC = 99% for segment length of 4097 samples. This ACC is obtained when $N_s = 12$ and NORF = 35. Since only twelve sub-bands are used in feature computation, there are 66 features available. Out of them, best 35 features provided ACC = 99%. The sub-bands used to compute these best features are shown in Table 2. In the Table 2, Cm is the feature having rank m and (a,b) denotes sub-band a and sub-band b which are used to compute feature Cm. The obtained SEN when obtained ACC = 99%, are $SEN_1 = 98.5\%$, $SEN_2 = 98\%$, and $SEN_3 = 100\%$. Similarly, the value of specificities $SPE_1 = 99.33\%$, $SPE_2 = 99.5\%$, and $SPE_3 = 99.67\%$.

It can be noted from Table 1 that, for other segment length also, the obtained ACC is at least 98%. However the number of features used for classification increases as the segment length decreases.

It can also be observed from Table 1 that the decrease in segment length decreases the ACC and increases the complexity of the system. Table 3 shows the comparison of the performance of ACC of proposed method with other existing methods using the same database (Andrzejak et al. 2001).

From this table, it can be observed that the proposed method obtained the better ACC as compared with other existing methods. The statistical analysis of computed features in (Tzallas et al. 2007; Peker et al. 2016; Tiwari et al. 2017; Bhattacharyya et al. 2017b), and proposed method are shown in Figs. 4, 5, 6, 7, and 8. The figures shows the mean and standard deviation (STD) of features for various methods. The mid point of the bar is the mean of the feature and half of the length of the bar is STD of feature when range of feature is shown in linear scale.

Table 1 Obtained ACC for different segment length

Segment length	ACC (%)	N_s	NORF
4097	99	12	35
2000	98.8	31	400
1000	98.2	39	715
500	98	39	741

Table 2 Sub-bands used to compute ranked features

Cm	(a,b)	Cm	(a,b)	Cm	(a,b)	Cm	(a,b)
C1	(3,12)	C10	(2,3)	C19	(9,11)	C28	(3,4)
C2	(3,11)	C11	(1,6)	C20	(4,12)	C29	(4,11)
C3	(3,10)	C12	(3,6)	C21	(2,11)	C30	(4,10)
C4	(3,9)	C13	(5,9)	C22	(1,8)	C31	(2,10)
C5	(1,7)	C14	(3,7)	C23	(4,9)	C32	(11,12)
C6	(1,11)	C15	(2,12)	C24	(1,5)	C33	(8,9)
C7	(1,12)	C16	(9,10)	C25	(5,12)	C34	(2,8)
C8	(3,8)	C17	(9,12)	C26	(2,9)	C35	(5,6)
C9	(1,10)	C18	(1,9)	C27	(5,11)		

Table 3 Summary of automated detection of seizure, seizure-free, and normal EEG signals using the same database

Authors	Features	Classifier	Training and testing data selection	ACC (%)
Tzallas et al. (2007)	SPWVD based features	ANN	50 % training and 50 % testing	97.72
Acharya et al. (2011a)	RQA features	SVM	3-fold cross-validation	95.6
Acharya et al. (2012)	ApE, SaE, and Phase entropy	Fuzzy	3-fold cross-validation	98.1
Peker et al. (2016)	Statistical features	Complex valued neural networks	10-fold cross-validation	98.28
Tiwari et al. (2017)	Histogram of LBP	SVM	10-fold cross-validation	98.8
Bhattacharyya et al. (2017b)	TQWT-based multi-scale K-NN entropy	SVM	10-fold cross-validation	98.6
Proposed method	CIP of sub-band signals from TQWT based filter-bank	RF	10-fold cross-validation	99

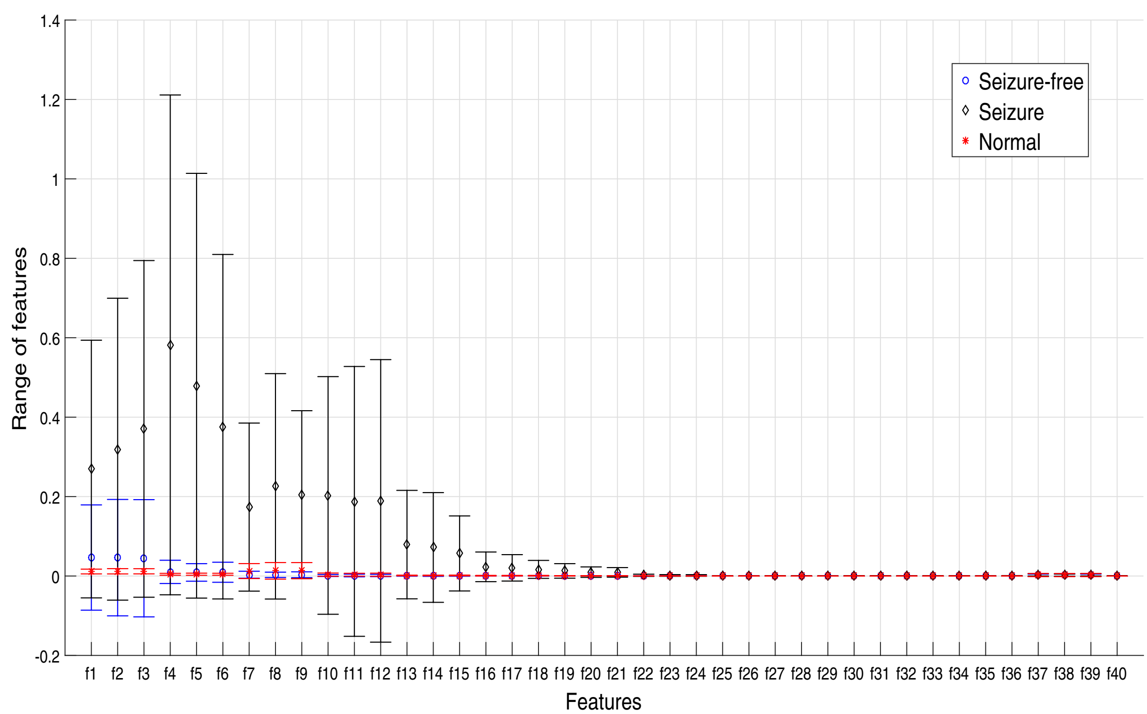

Fig. 4 Statistical analysis (mean and STD) of features computed in Tzallas et al. (2007)

7 Discussion

This paper presents a novel technique based on TQWT based filter-bank for the classification of epileptic EEG signals. The EEG signals are decomposed into narrow *BW* sub-band signals by TQWT based filter-bank and features are computed by applying CIP on every pair of sub-band signals. The CIP captures the similarity between two sub-band signals. To reduce the complexity of the proposed system, we have evaluated the optimal number of sub-band signals for computation of features instead of using all sub-band signals generated by TQWT based filter-bank. These features are then ranked using RELIEFF algorithm in order to obtain significant features. We found that $N_s = 12$, NORF = 35 with RF classifier yielded the maximum ACC = 99%.

The performance of proposed method in terms of obtained ACC is better than other existing methods as shown in Table 3. The features of EEG signals are analyzed using smoothed pseudo Wigner-Ville distribution (SPWVD) (Tzallas et al. 2007). The SPWVD is partitioned into different T–F planes. For partitioning, three time windows and thirteen frequency sub-bands are chosen (Tzallas et al. 2007). The time windows TW1, TW2, and TW3 are from 0 to 7.86 seconds, 7.86 to 15.73 seconds, and 15.73 to 23.6

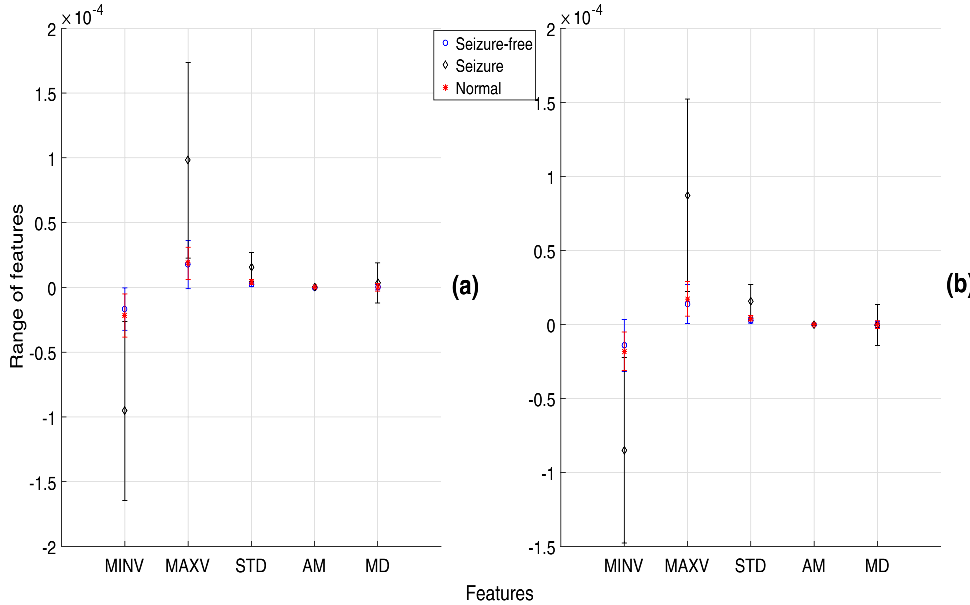

Fig. 5 Statistical analysis (mean and STD) of **a** real part of features and **b** imaginary part of features computed in Peker et al. (2016)

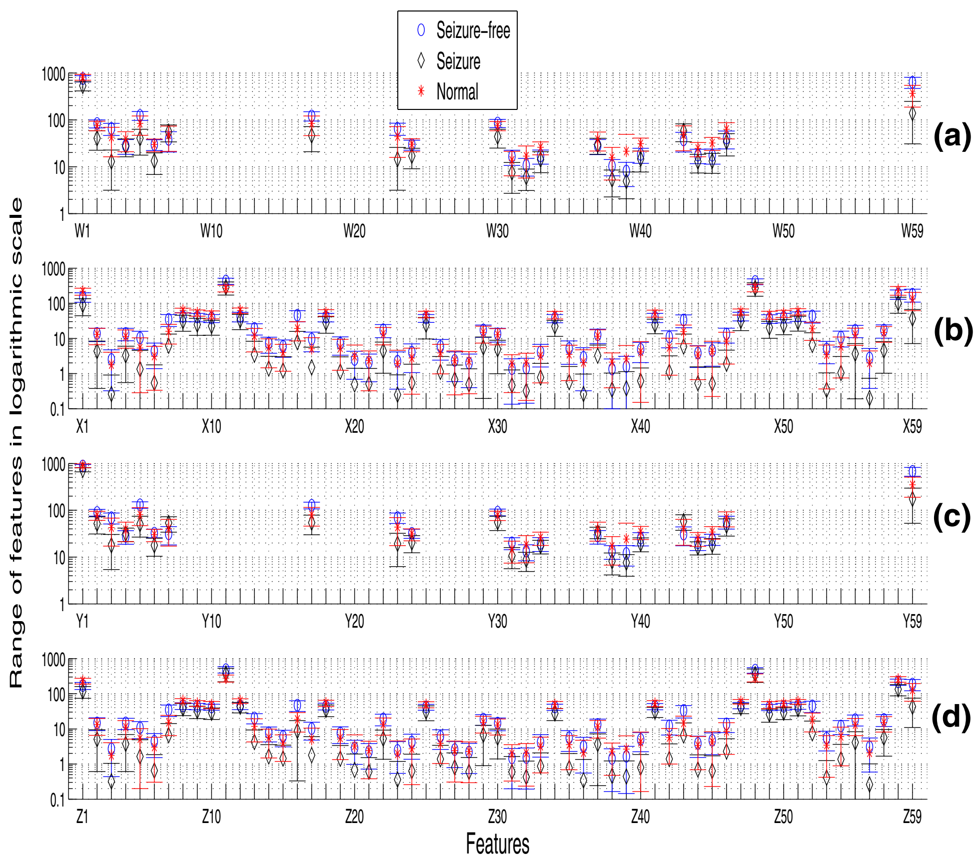

Fig. 6 Statistical analysis (mean and STD) of computed **a** W features, **b** X features, **c** Y features, and **d** Z features, in Tiwari et al. (2017)

seconds respectively (Tzallas et al. 2007). Similarly, the frequency windows FW1, FW2, FW3, FW4, FW5, FW6, FW7, FW8, FW9, FW10, FW11, FW12, and FW13 are from 0 to 2 Hz, 2 to 4 Hz, 4 to 6 Hz, 6 to 8 Hz, 8 to 10 Hz, 10 to 12 Hz, 12 to 16 Hz, 16 to 20 Hz, 20 to 24 Hz, 24 to 28 Hz, 28 to 32 Hz, 32 to 36 Hz, and 36 to 40 Hz respectively. The T–F plane TdFe is obtained by applying time window TWd and FWe where $1 \leq d \leq 3$ and $1 \leq e \leq 13$. The features f1, f2, f3, f4, f5, f6, f7, f8, f9, f10, f11, f12, f13, f14, f15, f16, f17, f18, f19, f20, f21, f22, f23, f24, f25, f26, f27, f28, f29, f30, f31,

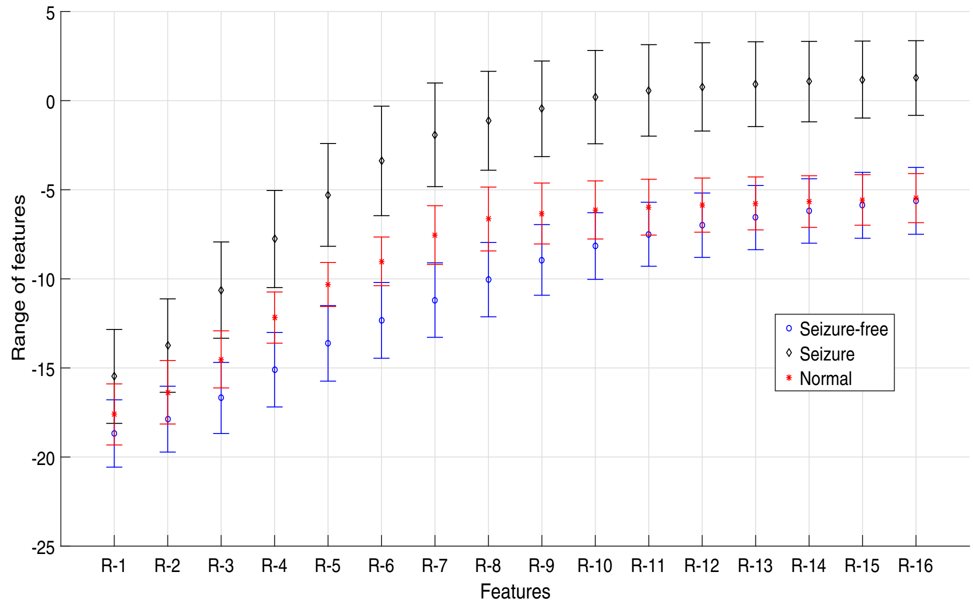

Fig. 7 Statistical analysis (mean and STD) of features computed in Bhattacharyya et al. (2017b)

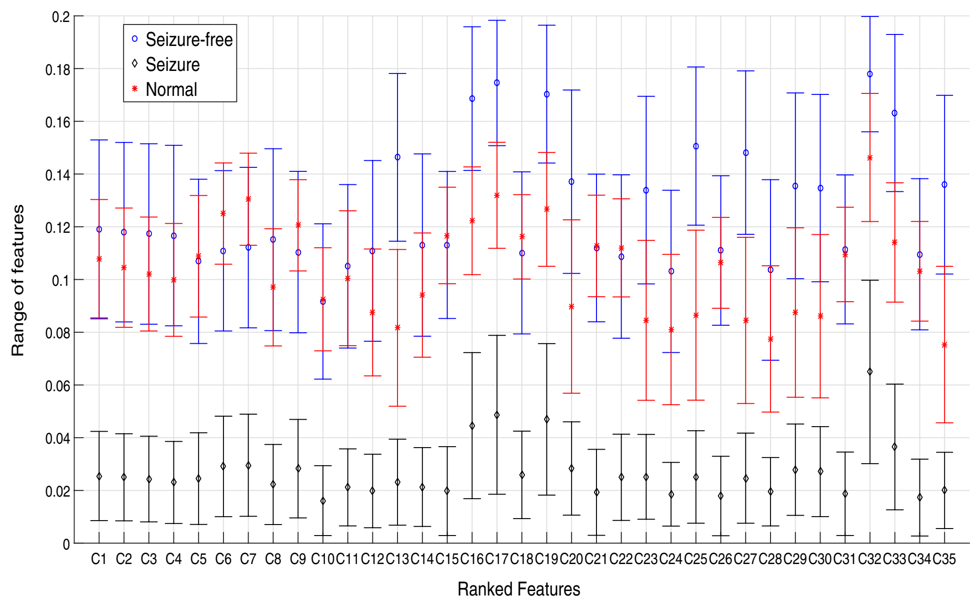

Fig. 8 Statistical analysis (mean and STD) of features computed in our proposed method

f32, f33, f34, f35, f36, f37, f38, and f39 are computed from T1F1, T2F1, T3F1, T1F2, T2F2, T3F2, T1F3, T2F3, T3F3, T1F4, T2F4, T3F4, T1F5, T2F5, T3F5, T1F6, T2F6, T3F6, T1F7, T2F7, T3F7, T1F8, T2F8, T3F8, T1F9, T2F9, T3F9, T1F10, T2F10, T3F10, T1F11, T2F11, T3F11, T1F12, T2F12, T3F12, T1F13, T2F13, and T3F13 respectively. They are shown in Fig. 4. The last feature f40 is the energy of EEG signal. Then energy features f1 to f39 are computed from their respective T–F plane (Tzallas et al. 2007). We implemented the proposed method in Tzallas et al. (2007) by using T–F toolbox available at (Auger et al. 1996). The statistical analysis of obtained features are shown in Fig. 4. It can be observed that mean of seizure EEG signal is notably far from mean of seizure-free and normal EEG signals for few features. The probability (p)-value of each feature is computed from Kruskal–Wallis test (McKight and Najab 2010). It is less than 0.05 for each feature.

In Acharya et al. (2011a), RQA method is employed. The features such as recurrence rate (RR), determinism (DET), mean diagonal line length (MDLL), longest diagonal line (LDL), entropy (E), laminarity (LM), trapping time (TT), longest vertical line (LVL), and recurrence times (T1 and T2) are used to classify the EEG signals. The mean ± STD of RR, DET, MDLL, LDL, E, LM, TT, LVL, T1, and T2 for normal EEG signals are 0.0575808 ± 0.004212, 0.26333 ± 0.04178, 2.3101 ± 0.112, 7.685 ± 1.5,

0.70126 ± 0.156, 0.35446 ± 0.05464, 2.402 ± 0.126, 7.195 ± 1.62, 16.383 ± 1.21, and 20.762 ± 1.32 respectively (Acharya et al. 2011a). Similarly for seizure-free class, the mean ± STD of RR, DET, MDLL, LDL, E, LM, TT, LVL, T1, and T2 are 0.0617364 ± 0.01391, 0.48499 ± 0.127, 2.6712 ± 0.668, 17.425 ± 26.6, 1.0463 ± 0.317, 0.61359 ± 0.124, 2.9401 ± 0.964, 12.47 ± 8.97, 15.159 ± 2.15, and 26.371 ± 4.57, respectively (Acharya et al. 2011a). For seizure EEG signals, the statistical analysis of RR, DET, MDLL, LDL, E, LM, TT, LVL, T1, and T2 are 0.0671869 ± 0.008863, 0.47018 ± 0.109, 3.0637 ± 0.417, 30.33 ± 16.1, 1.373 ± 0.238, 0.57155 ± 0.134, 3.2156 ± 0.535, 15.97 ± 7, 14.294 ± 1.78, and 24.509 ± 4.31 respectively (Acharya et al. 2011a). The $p-$values < 0.0001 for all features (Acharya et al. 2011a). The method proposed in Acharya et al. (2012) used phase entropies (S1 and S2), ApE, and SaE for classification. The mean ± STD of ApE, SaE, S1, and S2 for normal EEG signals are 2.2735 ± 0.0332, 1.313 ± 0.12, 0.57012 ± 0.0712, and 0.76827 ± 0.03125 respectively (Acharya et al. 2012). In the same way, the mean ± STD of ApE, SaE, S1, and S2 for seizure-free EEG signals are 1.865 ± 0.331, 0.99332 ± 0.189, 0.47208 ± 0.06149, and 0.68072 ± 0.0379, respectively (Acharya et al. 2012). For seizure EEG signals, the mean ± STD of ApE, SaE, S1, and S2 are 1.9325 ± 0.215, 0.92628 ± 0.139, 0.48325 ± 0.155, and 0.73184 ± 0.04555 respectively (Acharya et al. 2012). For all features in each class, the p-value is less than 0.0001 (Acharya et al. 2012).

The authors (Peker et al. 2016) used DTCWT to decompose input EEG signals. The decomposition by DTCWT generates complex wavelet coefficients. The computed features are minimum value (MINV), maximum value (MAXV), STD, arithmetic mean (AM), and median (MD). The Fig. 5a, b shows the statistical analysis of real and imaginary parts of the features respectively. We have implemented the method proposed in Peker et al. (2016) using matlab codes available at http://eeweb.poly.edu/iselesni/WaveletSoftware/ to implement DTCWT. The obtained p-values from Kruskal–Wallis test (McKight and Najab 2010) are less than 0.0001 for most of the features.

The statistical analysis of features computed using the method proposed in Tiwari et al. (2017) is shown in Fig. 6. In this method, the EEG signals are filtered by set of Gaussian filters having different STDs. Then the filtered EEG signals are subtracted to obtain pyramid of difference of Gaussian (DoG) filtered signals (Tiwari et al. 2017). From DoG signals, the local binary pattern (LBP) at key points are obtained according to the method proposed in (Tiwari et al. 2017). Finally, the histograms of LBP are taken as features and classified. In Tiwari et al. (2017), the set of key points K2 and K3 are computed from second and third signals of DoG pyramid respectively. In Fig. 6a features W1 to W59 are computed from second signal of DoG pyramid at K2. Similarly, features X1 to X59 as shown in Fig. 6b, are computed from the original EEG signal at K2. In Fig. 6c, d, features Y1 to Y59 are computed from third signal of DoG pyramid at K3 and features Z1 to Z59 are computed from original EEG signal at K3. There are few features whose mean and STD are zero for all classes. Therefore, in Fig. 6, the mean and STD of such features are not present as the range of features are shown in logarithmic scale. In this method, though the obtained ACC is high, the number of features used for classification is high. The features whose statistical analysis shown in Fig. 6 have p-values less than 0.0001. The p-values are computed from Kruskal–Wallis test (McKight and Najab 2010).

The authors (Bhattacharyya et al. 2017b) have proposed a multi-scale entropy based on Q-factor computed by decomposing EEG signal into sub-bands by TQWT. Then, from sub-bands, entropies based on K-NN, were estimated to classify epileptic EEG signals. The feature R- g is the K-NN entropy of reconstructed signal R (Bhattacharyya et al. 2017b). The reconstructed signal R is the summation of g sub-band signals obtained from sub-bands of TQWT (Bhattacharyya et al. 2017b). The statistical analysis of its features is shown in Fig. 7. Most of the features of seizure EEG signals are differentiable (distinct mean and STD values) from seizure-free and normal classes. For all features, $p-$value < 0.0001 [obtained from Kruskal–Wallis test (McKight and Najab 2010)]. The Fig. 8 shows the statistical analysis of features computed from proposed method. The proposed method obtained best ACC from 35 ranked features only when $N_s = 12$. The Fig. 8 shows the statistical analysis of these 35 ranked features. The mean and STD values of seizure EEG features is clearly separable from mean and STD of seizure-free and normal features. The mean and STD of few seizure-free and normal features are also clearly differentiable. The Kruskal–Wallis test (McKight and Najab 2010) is used to compute the p-values of all 35 features and they are less than 0.0001. This shows the statistical significance of features. This also implies that, the confidence interval is more than 95%.

The features computed in Tzallas et al. (2007); Acharya et al. (2011a, 2012); Tiwari et al. (2017); Bhattacharyya et al. (2017b), and proposed method, have p-value less than 0.05. Even in the proposed method, if all sub-bands of TQWT based filter-bank are used for feature computation, the obtained p-value of all computed features is below 0.05. This indicates that the computed features are statistically significant. Hence, the obtained ACC by these methods can also be viewed as a comparison of classification results using statistical test.

It can be observed from Figs. 4, 5, 6, 7, and 8, that in most of the cases, the mean and STD of seizure is easily distinguishable from mean and STD of seizure-free and normal

EEG signals. This is because during seizure activity, there is frequent spikes in EEG signal (Ray 1994; Mukhopadhyay and Ray 1998). Also the energy of seizure EEG signals are higher than the energy of seizure-free and normal EEG signals (Andrzejak et al. 2001). However, there may be some spikes in seizure-free EEG signals due undesirable artifacts or movement of muscles (Bhattacharyya and Pachori 2017). In such cases also, it may be difficult to differentiate seizure and seizure-free EEG signals.

The traditional machine technique is based on feature extraction from EEG signals and employing classifiers for the classification. However, it is difficult to choose the appropriate features to yield the maximum performance. In deep learning technique, the EEG signals are used as it is to develop the deep learning model without extracting the features for the classification (Faust et al. 2018; Rahhal et al. 2016). Recently, many authors have employed deep learning techniques for the automated detection of epilepsy (Acharya et al. 2018; Birjandtalab et al. 2017; Kornek et al. 2018). In future, we intend to explore these techniques to improve the classification of performance of the seizure.

8 Conclusion

The proposed work addresses the classification of seizure, seizure-free, and normal EEG signals which vary in their characteristics. The proposed technique explores this property in classifying EEG signals. The novelty of proposed method is the use of TQWT based filter-bank and CIP. The TQWT based filter-bank decomposes EEG signals into various sub-band signals. Then CIP captures the similarity from optimum number of sub-band signals and classifies in to seizure, seizure-free, and normal EEG signals. The obtained CIP values are different for various EEG signals. It has been observed that the mean of features for seizure, seizure-free, and normal EEG signals are differentiable in most of the cases. Thus, the obtained CIP values from proposed method influence the classification performance.

The proposed method computed the features from N_s selected sub-bands. The highest ACC of 99% is achieved by our proposed method. Also the computed features are statistically significant as p-value of all features is less than 0.0001. The limitation of the proposed method is that the number of features required increases parabolically as the number of sub-band signals increases and will boost the complexity of the system. The proposed method can aid the neurologists to detect epileptic seizures from EEG signals accurately. In future, deep learning can be employed for the diagnosis of epilepsy. This proposed TQWT based filter-bank method can be used detect focal, alcoholic and autistic, and Alzheimer's EEG signals.

Acknowledgements The authors would like to thank Prof. U. R. Acharya for his help during manuscript preparation. The authors are also thankful to Ashwani Kumar Tiwari and Abhijit Bhattacharyya for their help in providing MATLAB codes due to which we have shown the statistical analysis of features.

References

Accardo A, Affinito M, Carrozzi M, Bouquet F (1997) Use of the fractal dimension for the analysis of electroencephalographic time series. Biol Cybern 77:339–350

Acharya UR, Molinari F, Sree SV, Chattopadhyay S, Ng KH, Suri JS (2012) Automated diagnosis of epileptic EEG using entropies. Biomed Signal Process Control 7:401–408

Acharya UR, Yanti R, Zheng JW, Krishnan MMR, Tan JH, Martis RJ, Lim CM (2013) Automated diagnosis of epilepsy using CWT, HOS and texture parameters. Int J Neural Syst 23:1350009

Acharya UR, Oh SL, Hagiwara Y, Tan JH, Adeli H (2018) Deep convolutional neural network for the automated detection and diagnosis of seizure using EEG signals. Comput Biol Med 100:270–278

Acharya UR, Chua CK, Lim TC, Dorithy, Suri JS (2009) Automatic identification of epileptic EEG signals using nonlinear parameters. J Mech Med Biol 9:539–553

Acharya UR, Sree SV, Chattopadhyay S, Yu W, Ang PCA (2011a) Application of recurrence quantification analysis for the automated identification of epileptic EEG signals. Int J Neural Syst 21:199–211

Acharya UR, Sree SV, Suri JS (2011b) Automatic detection of epileptic EEG signals using higher order cumulant features. Int J Neural Syst 21:403–414

Adeli H, Zhou Z, Dadmehr N (2003) Analysis of EEG records in an epileptic patient using wavelet transform. J Neurosci Methods 123:69–87

Adeli H, Ghosh-Dastidar S, Dadmehr N (2007) A wavelet-chaos methodology for analysis of EEGs and EEG subbands to detect seizure and epilepsy. IEEE Trans Biomed Eng 54:205–211

Andrzejak RG, Lehnertz K, Mormann F, Rieke C, David P, Elger CE (2001) Indications of nonlinear deterministic and finite-dimensional structures in time series of brain electrical activity: dependence on recording region and brain state. Phys Rev 64:061907

Auger F, Flandrin P, Goncalves P, Lemoine O (1996) Time-frequency toolbox. CNRS France-Rice University

Azar AT, El-Said SA (2014) Performance analysis of support vector machines classifiers in breast cancer mammography recognition. Neural Comput Appl 24:1163–1177

Bajaj V, Pachori RB (2012) Classification of seizure and nonseizure EEG signals using empirical mode decomposition. IEEE Trans Inf Technol Biomed 16:1135–1142

Berger H (1929) Uber das elektroenkephalogramm des menschen. Arch Psychiatr Nervenkr 87:527–570

Bhati D, Pachori RB, Gadre VM (2017a) A novel approach for time-frequency localization of scaling functions and design of three-band biorthogonal linear phase wavelet filter banks. Digit Signal Proc 69:309–322

Bhati D, Sharma M, Pachori RB, Gadre VM (2017b) Time-frequency localized three-band biorthogonal wavelet filter bank using semidefinite relaxation and nonlinear least squares with epileptic seizure EEG signal classification. Digit Signal Proc 62:259–273

Bhattacharyya A, Pachori RB (2017) A multivariate approach for patient-specific EEG seizure detection using empirical wavelet transform. IEEE Trans Biomed Eng 64:2003–2015

Bhattacharyya A, Pachori RB, Acharya UR (2017a) Tunable-Q wavelet transform based multivariate sub-band fuzzy entropy with application to focal EEG signal analysis. Entropy 19:99

Bhattacharyya A, Pachori RB, Upadhyay A, Acharya UR (2017b) Tunable-Q wavelet transform based multiscale entropy measure for automated classification of epileptic EEG signals. Appl Sci 7:385

Birjandtalab J, Heydarzadeh M, Nourani M (2017) Automated EEG-based epileptic seizure detection using deep neural networks. In: Proceedings of IEEE International Conference on Healthcare Informatics (ICHI), pp 552–555

Boashash B, Colditz P, Mesbah M (2003) Time frequency detection of EEG abnormalities. Elsevier, Amsterdam

Breiman L (2001) Random forests. Mach Learn 45:5–32

Caton R (1875) The electric currents of brain. Br Med J 2:278

Chen G (2014) Automatic EEG seizure detection using dual-tree complex wavelet-Fourier features. Expert Syst Appl 41:2391–2394

Faust O, Hagiwara Y, Hong TJ, Lih OS, Acharya UR (2018) Deep learning for healthcare applications based on physiological signals: a review. Comput Methods Programs Biomed 161:1–13

Fraiwan L, Lweesy K, Khasawneh N, Wenz H, Dickhaus H (2012) Automated sleep stage identification system based on time-frequency analysis of a single EEG channel and random forest classifier. Comput Methods Programs Biomed 108:10–19

Ghosh-Dastidar S, Adeli H, Dadmehr N (2007) Mixed-band wavelet-chaos-neural network methodology for epilepsy and epileptic seizure detection. IEEE Trans Biomed Eng 54:1545–1551

Guler NF, Ubeyli ED, Guler I (2005) Recurrent neural networks employing Lyapunov exponents for EEG signals classification. Expert Syst Appl 29:506–514

Guo L, Rivero D, Pazos A (2010) Epileptic seizure detection using multiwavelet transform based approximate entropy and artificial neural networks. J Neurosci Methods 193:156–163

Hall M, Frank E, Holmes G, Pfahringer B, Reutemann P, Witten IH (2009) The WEKA data mining software: an update. SIGKDD Explorations 11:10–18

Hassan AR, Siuly S, Zhang Y (2016) Epileptic seizure detection in EEG signals using tunable-Q factor wavelet transform and bootstrap aggregating. Comput Methods Programs Biomed 137:247–259

Huang NE, Shen Z, Long SR (1999) new view of nonlinear water waves: the Hilbert spectrum. Annu Rev Fluid Mech 31:417–457

Khan YU, Gotman J (2003) Wavelet based automatic seizure detection in intracerebral electroencephalogram. Clin Neurophysiol 114:898–908

Kononenko I, Simec E, Robnik-Sikonja M (1997) Overcoming the myopia of inductive learning algorithms with RELIEFF. Applied Intelligence 7:39–55

Kornek IK, Roy S, Nurse E, Mashford B, Karoly P, Carroll T, Payne D, Saha S, Baldassano S, O'Brien T, Grayden D, Cook M, Freestone D, Harrer S (2018) Epileptic seizure prediction using big data and deep learning: toward a mobile system. EBioMedicine 27:103–111

Kumar M, Pachori RB, Acharya UR (2017) Characterization of coronary artery disease using flexible analytic wavelet transform applied on ECG signals. Biomed Signal Process Control 31:301–308

Lee SH, Lim JS, Kim JK, Yang J, Lee Y (2014) Classification of normal and epileptic seizure EEG signals using wavelet transform, phase-space reconstruction, and Euclidean distance. Comput Methods Programs Biomed 116:10–25

Lehnertz K, Elger CE (1995) Spatio-temporal dynamics of the primary epileptogenic area in temporal lobe epilepsy characterized by neuronal complexity loss. Electroencephalogr Clin Neurophysiol 95:108–117

Liang SF, Wang HC, Chang WL (2010) Combination of EEG complexity and spectral analysis for epilepsy diagnosis and seizure detection. EURASIP J Adv Signal Process 2010:853434

McKight PE, Najab J (2010) Kruskal-Wallis Test. Corsini Encyclopedia of Psychology

Mukhopadhyay S, Ray GC (1998) A new interpretation of nonlinear energy operator and its efficacy in spike detection. IEEE Trans Biomed Eng 45:180–187

Nishad A, Pachori RB, Acharya UR (2018) Application of TQWT based filter-bank for sleep apnea screening using ECG signals. J Ambient Intell Hum Comput. https://doi.org/10.1007/s12652-018-0867-3

Ocak H (2009) Automatic detection of epileptic seizures in EEG using discrete wavelet transform and approximate entropy. Expert Syst Appl 36:2027–2036

Orhan U, Hekim M, Ozer M (2011) EEG signals classification using the K-means clustering and a multilayer perceptron neural network model. Expert Syst Appl 38:13475–13481

Oweis RJ, Abdulhay EW (2011) Seizure classification in EEG signals utilizing Hilbert-Huang transform. BioMedical Eng OnLine 10:38

Pachori RB (2008) Discrimination between ictal and seizure-free EEG signals using empirical mode decomposition. Res Lett Signal Process 2008:1–5

Pachori RB, Bajaj V (2011) Analysis of normal and epileptic seizure EEG signals using empirical mode decomposition. Comput Methods Programs Biomed 104:373–381

Pachori RB, Nishad A (2016) Cross-terms reduction in the Wigner–Ville distribution using tunable-Q wavelet transform. Sig Process 120:288–304

Pachori RB, Patidar S (2014) Epileptic seizure classification in EEG signals using second-order difference plot of intrinsic mode functions. Comput Methods Programs Biomed 113:494–502

Pachori RB, Sharma R, Patidar S (2015) Classification of normal and epileptic seizure EEG signals based on empirical mode decomposition. Springer, Berlin

Patidar S, Panigrahi T (2017) Detection of epileptic seizure using Kraskov entropy applied on tunable-Q wavelet transform of EEG signals. Biomed Signal Process Control 34:74–80

Patidar S, Pachori RB, Acharya UR (2015a) Automated diagnosis of coronary artery disease using tunable-Q wavelet transform applied on heart rate signals. Knowl-Based Syst 82:1–10

Patidar S, Pachori RB, Garg N (2015b) Automatic diagnosis of septal defects based on tunable-Q wavelet transform of cardiac sound signals. Expert Syst Appl 42:3315–3326

Patidar S, Pachori RB, Upadhyay A, Acharya UR (2017) An integrated alcoholic index using tunable-Q wavelet transformbased features extracted from EEG signals for diagnosis of alcoholism. Appl Soft Comput 50:71–78

Peker M, Sen B, Delen D (2016) A novel method for automated diagnosis of epilepsy using complex-valued classifiers. IEEE J Biomed Health Inf 20:108–118

Polat K, Gunes S (2007) Classification of epileptiform EEG using a hybrid system based on decision tree classifier and fast Fourier transform. Appl Math Comput 187:1017–1026

Rahhal MMA, Bazi Y, AlHichri H, Alajlan N, Melgani F, Yager RR (2016) Deep learning approach for active classification of electrocardiogram signals. Inf Sci 345:340–354

Ray GC (1994) An algorithm to separate nonstationary part of a signal using mid-prediction filter. IEEE Trans Signal Process 42:2276–2279

Robnik-Sikonja M, Kononenko I (2003) Theoretical and empirical analysis of ReliefF and RReliefF. Mach Learn 53:23–69

Samiee K, Kovacs P, Gabbouj M (2015) Epileptic seizure classification of eeg time-series using rational discrete short-time fourier transform. IEEE Trans Biomed Eng 62:541–552

Selesnick IW (2011a) TQWT toolbox guide. Electrical and Computer Engineering Polytechnic Institute of New York University

Selesnick IW (2011b) Wavelet transform with tunable Q-factor. IEEE Trans Signal Process 59:3560–3575

Sharma M, Pachori RB (2017) A novel approach to detect epileptic seizures using a combination of tunable-Q wavelet transform and fractal dimension. J Mech Med Biol 17:1740003

Sharma R, Pachori RB (2015) Classification of epileptic seizures in EEG signals based on phase space representation of intrinsic mode functions. Expert Syst Appl 42:1106–1117

Sharma R, Kumar M, Pachori RB, Acharya UR (2017) Decision support system for focal EEG signals using tunable-Q wavelet transform. J Comput Sci 20:52–60

Sharma RR, Pachori RB (2018) Time-frequency representation using IEVDHM-HT with application to classification of epileptic EEG signals. IET Sci Meas Technol 12:72–82

Srinivasan V, Eswaran C, Sriraam N (2005) Artificial neural network based epileptic detection using time-domain and frequency-domain features. J Med Syst 29:647–660

Subasi A (2007) EEG signal classification using wavelet feature extraction and a mixture of expert model. Expert Syst Appl 32:1084–1093

Subasi A, Gursoy MI (2010) EEG signal classification using PCA, ICA, LDA and support vector machines. Expert Syst Appl 37:8659–8666

Tiwari AK, Pachori RB, Kanhangad V, Panigrahi BK (2017) Automated diagnosis of epilepsy using key-point-based local binary pattern of EEG Signals. IEEE J Biomed Health Inf 21:888–896

Tzallas AT, Tsipouras MG, Fotiadis DI (2009) Epileptic seizure detection in EEGs using time–frequency analysis. IEEE Trans Inf Technol Biomed 13:703–710

Tzallas AT, Tsipouras MG, Fotiadis DI (2007) Automatic seizure detection based on time-frequency analysis and artificial neural networks. Comput Intell Neurosci 2007:1–13

Ubeyli ED (2010) Lyapunov exponents/probabilistic neural networks for analysis of EEG signals. Expert Syst Appl 37:985–992

Witte H, Iasemidis LD, Litt B (2003) Special issue on epileptic seizure prediction. IEEE Trans Biomed Eng 50:537–539

Xu D, Erdogmuns D (2010) Renyi's entropy, divergence and their nonparametric estimators. Springer, New York, pp 47–102

Xu JW, Paiva ARC, Park II, Principe JC (2008) A reproducing kernel Hilbert space framework for information-theoretic learning. IEEE Trans Signal Process 56:5891–5902

Publisher's Note Springer Nature remains neutral with regard to jurisdictional claims in published maps and institutional affiliations.